

**BUBBLE ATTACHMENT TIME AND FTIR ANALYSIS OF WATER
STRUCUTRE IN THE FLOTATION OF SYLVITE, BISCHOFITE
AND CARNALLITE**

**Qinbo Cao¹, Xuming Wang^{2*}, Jan D Miller², Fangqin Cheng^{1,3*} and
Yong Jiao¹**

¹ Research Center for Environmental Science and Engineering, Shanxi University, No 92 Wucheng Road, Taiyuan, Shanxi 030006, China

² Department of Metallurgical Engineering, College of Mines and Earth Sciences, University of Utah, 135S 1460E 412 WBB, Salt Lake City, UT 84112, U.S.A.

³ Department of Chemical Engineering, Qinhai University, No 251 Ning Road, Xining, Qinhai 810016, China

* To whom correspondence should be addressed.

Xuming Wang

Fax: 801-5814937. E-mail: x.wang@utah.edu

Fangqin Cheng

Fax: 86 03517016893. E-mail: cfangqin@sxu.edu.cn

BUBBLE ATTACHMENT TIME AND FTIR ANALYSIS OF WATER STRUCTURE IN THE FLOTATION OF SYLVITE, BISCHOFITE AND CARNALLITE

Qinbo Cao, Xuming Wang, Jan D Miller, Fangqin Cheng and Yong Jiao

ABSTRACT

Water structure is a most important parameter that influences the flotation of soluble salts. In this paper bubble attachment time measurements and FTIR analyses were performed to investigate the effect of water structure on the flotation behavior of sylvite (KCl), bischofite ($\text{MgCl}_2 \cdot 6\text{H}_2\text{O}$) and carnallite ($\text{KMgCl}_3 \cdot 6\text{H}_2\text{O}$). The results from bubble attachment time measurements suggest that collector adsorption at the surface of KCl induces flotation with either the cationic collector, ODA or anionic collector, SDS. In contrast bubble attachment did not occur for bischofite ($\text{MgCl}_2 \cdot 6\text{H}_2\text{O}$) or carnallite ($\text{KMgCl}_3 \cdot 6\text{H}_2\text{O}$). Results show that the surface charge is not a determining factor in the flotation of soluble salts.

Further, the interaction between water molecules and the three chloride salts dissolved in aqueous solution were studied by measuring the shift in the hydrogen bonding of water molecules. The results indicate that KCl is a structure breaker salt, while $\text{MgCl}_2 \cdot 6\text{H}_2\text{O}$ and $\text{KMgCl}_3 \cdot 6\text{H}_2\text{O}$ are structure maker salts.

Viscosities for the brines of these three salts were determined. The results give additional evidence of differences in water structure and are in good agreement with the FTIR and bubble attachment results. The findings provide further evidence that water structure plays an important role in the flotation of soluble salts.

Keywords: *soluble salts, FTIR, O-D band, water structure, bubble attachment time, sylvite, bischofite, carnallite*

1. INTRODUCTION

The separation of sylvite from halite by flotation is well established and such sylvite ores are ideal for the production of potash. However, in some cases these preferred sylvite ores have been depleted. For example in the Permian Basin, New Mexico, low-grade ores containing carnallite ($\text{KMgCl}_3 \cdot 6\text{H}_2\text{O}$) and bischofite ($\text{MgCl}_2 \cdot 6\text{H}_2\text{O}$) are becoming the future source for potash production (Foot and Huiatt, 1981; Huiatt et al., 1975). At the Dead Sea Works, carnallite produced from solar ponds in Israel and Jordan is a major source for potash production. Carnallite is the next mineral predicted to precipitate in the Dead Sea (García-Veigas et al., 2009). It is apparent that carnallite is becoming an important resource for the production of potash.

Most marketable potash is produced by a) flotation, b) selective dissolution, and c) crystallization of potash minerals from saturated brines (hot leaching method) (Titkov, 2004). Among these methods, selective flotation with C12–C18 long-chain primary amines was first reported for the separation of KCl from other soluble salts in 1936 (Kirby, 1936) and from that time has been widely used to concentrate potash ores. Now, over 80% of world's potash is produced by selective flotation using primary amines as the collector (Searls, 1990).

Despite the successful commercial application of KCl flotation, the mechanism of flotation is still not completely understood. In the past six decades, many researchers suggested several models to explain the mechanism of soluble salt flotation (Du et al., 2008; Du et al., 2007; Fuerstenau and Fuerstenau, 1956; Hancer et al., 2001; Hancer and Miller, 2000; Miller et al., 1992; Rogers, 1957; Roman et al., 1968; Yalamanchili et al., 1993). The collector colloid/surface charge adsorption hypothesis is a classic explanation for primary amine flotation of alkali halides and the flotation behavior of KCl in particular (Miller et al., 1992; Roman et al., 1968; Yalamanchili et al., 1993). According to this model, the flotation behavior of soluble salts depends on the electrostatic interaction between the salt surface and the collector species. The flotation of KCl may be achieved by the adsorption of the cationic amine collector at the negatively charged KCl surface to create a hydrophobic surface. At the same time, the positively charged NaCl surface does not adsorb the cationic amine collector and remains hydrophilic. Because of the high solubility of soluble salts, the flotation process has to be carried out in saturated brines. The electrical double layer around the salt particles is highly compressed due to the high ionic strength of the saturated brine. So, direct determination of the sign of the surface charge is not possible by traditional zeta potential measurements. However in 1992, it was demonstrated that nonequilibrium electrophoretic mobility of soluble salts particles could be measured by laser-Doppler electrophoresis (Miller et al., 1992), which results provided experimental evidence of the surface charge. Later these data were support by the results from molecular dynamics simulations. Such reports

support the collector colloid/surface charge adsorption model. However, further research found that this model could not explain the fact that negatively charged KCl floats well or even better with the anionic collector sodium dodecylsulfate (SDS) (Hancer et al., 2001; Rogers, 1957).

The flotation mechanism of soluble salts can be better explained considering the hydration phenomena of salt surfaces, which was first suggested by Rogers and Schulman (Rogers, 1957). This model was further developed by Miller et al. in terms of interfacial water structure (Du et al., 2008; Du et al., 2007; Hancer et al., 2001; Nickolov et al., 2003; Ozdemir et al., 2007). In liquid water, at any moment in time, more than 75% of the molecules are interconnected in a three-dimensional network of three or four nearest neighbors through hydrogen bonds (Robinson et al., 1996). This network of water molecules can be described as the water structure. In saturated solutions of soluble salts, the water structure in the bulk solution and at the interface appears to be modified by the high concentration of dissolved ions. Depending on the effect of ions on the water structure, soluble salts can be classified into water structure breakers and water structure makers. Structure makers which enhance the H-bonding of water molecules and increase the “ice-like” structure in solution also stabilize the interfacial water at the salt/brine interface. As a result, it is impossible for either cationic or anionic collectors to penetrate the interfacial water film and adsorb at the salt crystal surface (Du et al., 2008; Du et al., 2007; Hancer et al., 2001). On other hand, structure breaker salts tend to decrease the fraction of tetrahedrally bonded water molecules and disrupt the organized water structure, which facilitates the adsorption of surfactant at such salt surfaces to create a hydrophobic state for the flotation of these salts (Du et al., 2008; Du et al., 2007; Hancer et al., 2001).

The classification of salts into water structure makers or water structure breakers is a very simplified approach to describe the water structure property as influenced by salt concentration (Du and Miller, 2007; Koneshan et al., 1998), but still is a convenient first order approximation. Traditionally, the viscosity of solutions is measured to investigate water structure characteristics (Hancer et al., 2001; Jiang and Sandler, 2003; Ozdemir et al., 2007). Structure makers increase the viscosity of the aqueous solution, while, structure breakers have the opposite influence. Sessile drop contact angle measurements have also been performed as a measure of the interfacial water structure. In the case of structure making salts, the surface is completely wetted by the brine and no contact angle can be measured. In the case of structure breaking salts, the brine does not completely wet the salt surface resulting in a finite contact angle (Hancer et al., 2001). Both viscosity and contact angle measurements are macro parameters of water structure properties in bulk solution and at the surface of salt crystals.

Vibrational spectroscopy (IR and Raman) has been used successfully to study



hydrogen-bonding in aqueous solutions, and provide direct evidence of the water structure making/breaking properties of salts at the molecular level (Dillon and Dougherty, 2002; Max and Chapados, 2007; Max and Chapados, 2005; Ujike et al., 1999). Usually, the attenuated total reflection (ATR) method is used to record the IR spectra of aqueous solutions (Nicholov et al., 2004; Nickolov et al., 2003). However, interfacial spectra in the OH stretching region are highly dependent on the optical constants of the total internal reflection element (Hancer et al., 2000). In addition, the spectra may be strongly distorted by the anomalous dispersion due to the dissolution/crystallization at the salt surface. So, it is difficult to directly analyze water structure at salt surfaces with this method. In 1987, sum frequency generation spectroscopy (SFG) was first introduced (Zhu et al., 1987) and then used to determine the vibrational spectra at interfaces, such as solid/liquid and liquid/air interfaces (Du et al., 2008). This method has been shown to be intrinsically surface sensitive, since such signals are forbidden in a bulk medium with inversion symmetry, but are available at a surface or interface where the inversion symmetry is broken. For example, at a solid/liquid interface, interfacial water with partially ordered structure can always be expected to appear in the SFG spectra while bulk water will have no signal. Thus, the water structure at a solid surface can be successfully detected by SFG spectroscopy. However, in the case of soluble salt systems, the high solubility of salt and the dissolution/crystallization at the salt surface make it difficult to measure the interfacial water structure by SFG spectra.

It is difficult to detect the interfacial water spectra in soluble salt systems by SFG, and the sampling volume is too large for FTIR-ATR spectroscopy. In this work, transmission FTIR was chosen to study the O–D stretching band in solutions of salts dissolved in 4 wt% D₂O/H₂O mixtures. Compared to SFG and FTIR-ATR techniques, this method has two advantages. First, when a small amount of D₂O is mixed with H₂O, HOD molecules are formed in solution due to the rapid exchange between H and D atoms. Because of the difference in atomic weight between the H and D atoms, coupling between O–D and O–H oscillators in HOD molecules is not possible. In addition, the intermolecular interactions between the two O–H oscillators in H₂O molecules do not complicate the O–H stretching band contour. As a result, the O–D band reflects only the hydrogen bonding interactions of the HOD molecules with all other water molecules (Zhelyaskov et al., 1988a, b). Second, since a small amount of D₂O is added to the H₂O, there are not so many HOD molecules in solution. So the O–D band absorption intensity is small enough to obtain a full O–D band shape in the transmission spectra when the concentrations of salts are varied from very dilute to saturated. Even in a saturated solution, the O–D band shape can be fully recorded with this method. Water structure analysis at these concentrations helps to understand the influence of soluble salts on water structure in the bulk solution, and which structure is also expected to arise at the surface of a salt crystal in its brine. In both bulk solutions and at the interface water structure will be influenced by the salt and its

concentration.

The objective of the present study is, therefore, to investigate the effect of water structure on the flotation of selected alkali halide salt minerals: KCl, $\text{MgCl}_2 \cdot 6\text{H}_2\text{O}$ and $\text{KMgCl}_3 \cdot 6\text{H}_2\text{O}$. Bubble attachment time experiments have been conducted to better understand the expected flotation response of these salts with dodecylsulfate (SDS) and 1-octadecylamine-HCl (ODA). FTIR transmission experiments have been carried out on the water structure making and breaking properties of these salt solutions at the molecular level. The structure making/breaking characteristics of these salts are further determined by measurements of the salt solution viscosity.

2. MATERIALS AND METHODS

2.1 Reagents and Materials

Potassium chloride (KCl), and magnesium chloride hexahydrate ($\text{MgCl}_2 \cdot 6\text{H}_2\text{O}$) used in this study were of reagent grade purchased from Sigma Aldrich company. 1-octadecylamine-HCl (ODA) with purity of 99.2% and sodium dodecyl-sulfate (SDS), purity 99%, were purchased from Fluka and Eastman Kodak respectively. These reagents were used without any further purification. Millipore water (18 $\text{M}\Omega\text{-cm}$) was used in all the experiments. All the glassware was soaked in chromic acid, rinsed with purified water and dried prior use.

The preparation of the saturated salt solution is very important because the solubility of the salt is highly dependent on temperature. In terms of KCl and $\text{MgCl}_2 \cdot 6\text{H}_2\text{O}$, a sufficient amount of each salt was dissolved in Millipore water and stirred overnight to achieve saturation. Then the saturated brines were stored for another 12 hours and filtered. Concerning carnallite ($\text{KMgCl}_3 \cdot 6\text{H}_2\text{O}$), according to the $\text{MgCl}_2\text{-KCl-H}_2\text{O}$ phase diagram at 25 °C (Cheng et al., 2002), 1.10g KCl and 74.79g $\text{MgCl}_2 \cdot 6\text{H}_2\text{O}$ should dissolve completely with 24.11g H_2O to obtain a saturated solution of carnallite. The carnallite was crystallized through evaporation of the carnallite saturated brine at room temperature.

2.2 Bubble Attachment Time Measurements

The MCT-100 Electronic Induction Timer was used to measure the bubble attachment time at the surfaces of KCl, $\text{MgCl}_2 \cdot 6\text{H}_2\text{O}$ and $\text{KMgCl}_3 \cdot 6\text{H}_2\text{O}$ salt particles with ODA and SDS. First, a desired amount of collector was added to the saturated brines of the selected salts. Then, 1g of salt sample (80x100 mesh) was added to the saturated solution with collectors and the suspension was stirred for 15 minutes to establish equilibrium in the induction timer cell. The mixture was settled for another 5 minutes to form a stable

particle bed before measurement. Finally, the cell containing the collector solution and particle bed was placed into the measurement chamber (Ye et al., 1989).

All the measurements were performed at room temperature and natural pH. In each test, an air bubble with 3mm diameter was generated by a micro syringe. Then the distance between the air bubble and particle bed was adjusted by the micro-scale of the microscope. The bubble was brought down to contact the surface of the particle bed at a specified contact time automatically controlled by the measurement machine. After that, whether or not particles attached to the air bubble was determined by observation through a microscope. Any particle attached to the air bubble surface was defined as an attachment event. A set of 20 measurements were performed at different places on the particle bed and the observations were recorded. The number of observations with attachment was divided by the total number of observations and recorded. Bubble attachment time is the time at which 50% of the contacts result in successful attachment.

2.3 FTIR Spectroscopy Measurement

The FTIR transmission spectra of brines were recorded in the range 300-4000 cm^{-1} on a Bio-Rad 6000 FTIR spectrometer with a broadband MCT detector. A cell with two CaF_2 windows and a 0.05 cm Teflon spacer was used in this study. All the spectra were recorded at room temperature by co-addition of 1024 interferograms at a resolution of 2 cm^{-1} and data points spacing 0.964 cm^{-1} .

The FTIR transmission spectra of the three salt solutions dissolved in 4 wt. % D_2O in H_2O mixtures, and in pure water were recorded respectively at the same spectrometer settings. The O-D stretching band between 2150-2750 cm^{-1} was analyzed. The spectrum of the O-D bands was obtained by spectral subtraction of the spectrum of the salt in pure water from those in the 4 wt. % $\text{D}_2\text{O}/\text{H}_2\text{O}$ mixtures. Then all the spectra were baseline corrected and normalized to unity in order to get a better comparison between the shapes of the O-D band at different concentrations.

2.4 Viscosity Analysis

The viscosity of MgCl_2 solutions at different concentrations was measured at room temperature. An Ubbelohde Viscometer with an estimated accuracy of $\pm 0.1\%$ purchased from the Cannon Instrument Co. was used for the viscosity measurements. The cell for measurement was cleaned in the order of acetone/methanol/pure water. The viscometer was cleaned by chromic acid and pure water. All the solutions were filtered with a 0.02- μm filter before measurement. Each test was performed three times and the mean value was recorded. The variation of results for each measurement was less than 0.02 cSt.

3. RESULTS AND DISCUSSION

3.1 Bubble Attachment Time Measurements

Flotation separation is controlled by the selected adsorption of collector molecules at mineral surfaces to establish a hydrophobic state. So, hydrophobic particles attach to air bubbles dispersed throughout the suspension and are recovered in the froth phase during flotation. Both the hydration state of the mineral surface and the selective adsorption of the collector are important issues in the study of flotation chemistry. Usually, contact angle and bubble attachment time experiments are performed to examine the hydrophobicity of mineral surfaces (Drelich et al., 1996; Ye et al., 1989; Ye and Miller, 1989). The contact angle is generally an equilibrium measurement of hydrophobicity, while the bubble attachment time is a kinetic measurement of the hydrophobicity. In some cases, the contact angle might fail to describe the flotation behavior (Finch and Smith, 1972; Lai and Smith, 1966; Rosenbaum et al., 1983). So, in this study, bubble attachment time was used to study the hydrophobicity of KCl, $\text{MgCl}_2 \cdot 6\text{H}_2\text{O}$ and $\text{KMgCl}_3 \cdot 6\text{H}_2\text{O}$ with ODA and SDS as collectors. The results for KCl are shown in Fig. 1 and Fig. 2.

The bubble attachments for KCl with different ODA and SDS concentrations are shown in Fig. 1 and Fig. 2 respectively. The results clearly show that, in the case of KCl, the attachment time decreased significantly with increasing ODA and SDS concentration. It is interesting to notice that when the concentration of ODA increased to 1×10^{-5} mol/L from 1×10^{-6} mol/L, the attachment time dramatically reduced. The concentration of 1×10^{-5} mol/L ODA is close to the precipitation concentration of ODA in KCl saturated KCl brine. The attachment time for KCl with ODA is much shorter than SDS at the same concentration, as seen from Table 1. For instance, the attachment time of KCl is 50ms for 1×10^{-5} mol/L ODA while 100 ms for SDS at the same concentration. It appears that ODA is more effective than SDS to make the KCl crystal surface sufficiently hydrophobic for bubble attachment.

The attachment results are in good agreement with previous microflotation results [13, 38]. It appears that the floatability of KCl with SDS is initiated at 8×10^{-6} mol/L. At this concentration, the attachment time of KCl with SDS is 190 ms. In the case of ODA, the attachment time decreases significantly from 600 ms to 60 ms when the concentration increases from 5×10^{-6} mol/L to 8×10^{-6} mol/L. The flotation recoveries are about 45% and 90% respectively at these concentrations (Cao et al., 2010). It should be noted that when the concentration of ODA is around 8×10^{-6} mol/L, precipitation of ODA occurs in the KCl saturated brine. It is much easier for the collector colloid to adsorb at the

liquid/air interface than at the solid/liquid interface, so air bubbles generated in the flotation cell, carry the collector colloid species and facilitate flotation (Burdukova and Laskowski, 2009; Burdukova et al., 2009).

In the case of SDS, the attachment time is 1800 ms at 1×10^{-6} mol/L, which does not change much compared to 2000 ms with no collector. As seen from previous studies (Cao et al., 2010; Hancer et al., 2001), the recovery of KCl with SDS is nearly zero at 1×10^{-6} mol/L. About 20% recovery is obtained at 8×10^{-6} mol/L (Cao et al., 2010).

The bubble attachment time results suggest that both ODA and SDS adsorb at the KCl crystal surface and provide a hydrophobic state for bubble/particle attachment. According to the surface charge model (Veeramasuneni et al., 1997), anionic collectors should not adsorb at the surface of a fine KCl crystal which is negatively charged in its saturated brine. However, both cationic and anionic collectors adsorb at the KCl crystal surface. Reports of previous contact angle and microflotation measurements also reached the same conclusion (Cao et al., 2010; Hancer et al., 2001). The results from both bubble attachment experiments and microflotation tests indicate that surface charge is not a determining factor in the flotation of KCl.

In addition, it should be noted that 50% attachment was observed at 2000 ms for KCl in the absence of collector. This result indicates the KCl surface shows a certain natural hydrophobicity, which agrees well with results of contact angle measurements reported in Hancer's earlier research (Hancer et al., 2001). There was no attachment observed for $\text{MgCl}_2 \cdot 6\text{H}_2\text{O}$ and $\text{KMgCl}_3 \cdot 6\text{H}_2\text{O}$ even at higher collector concentrations (5×10^{-5} mol/L) of both collectors. These results can be understood from the perspective of interfacial water structure. In the case of KCl, due to the weaker interaction of surface ions with water molecules, the arrangement of water molecules at the interface is less structured, less ordered, which facilitates the adsorption of collector. While in the case of $\text{MgCl}_2 \cdot 6\text{H}_2\text{O}$ and $\text{KMgCl}_3 \cdot 6\text{H}_2\text{O}$, a more stable hydration state is formed, compared to KCl at the crystal surface, and the surface is completely wetted by water. There appears to be a layer of stable interfacial water existing at the crystal/brine interface. The highly ordered water prevents collector adsorption for bischofite and carnallite.

In order to obtain more information about the interaction of these salts with water, FTIR-transmission spectroscopy experiments and viscosity measurements were made.

3.2 FTIR Spectroscopy Study

The results from the bubble attachment time measurements and the results from previous microflotation experiments show that KCl floats well with both the cationic collector ODA and the anionic collector SDS, while bischofite, $\text{MgCl}_2 \cdot 6\text{H}_2\text{O}$, and carnallite,

$\text{KMgCl}_3 \cdot 6\text{H}_2\text{O}$, cannot be floated with either collector. These results and the results from other researchers (Cao et al., 2010; Du et al., 2008; Hancer et al., 2001; M.Hancer.M.S.Celik., 2001) support the hypothesis that the degree of ion hydration is the determining factor for the flotation of soluble salts rather than surface charge or other phenomena. It seems that the flotation mechanism is better understood based on water structure theory.

Usually, changes of the H-bonding bands between 3000 and 3800 cm^{-1} are used to identify changes in water structure. The region around 3200 cm^{-1} is attributed to tetrahedrally bonded, ‘ice-like’ water molecules, while the region around 3400 cm^{-1} corresponds to molecules with a distorted, intermediate bond of H bonding (Scherer et al., 1974). The water structure also can be measured by the analysis of the O-D stretching band. In this work, the O-D stretching band between 2150 and 2750 cm^{-1} is analyzed. The region around 2380 cm^{-1} is for the ice-like water, while 2530 cm^{-1} is for incomplete tetrahedral coordination of water. It is well known that water structure maker salts increase the width of the O-D band and shift the peak position to the lower wavenumber side, while structure breaker salts decrease the width of the O-D band and shift the peak position to the higher wavenumber side (Nickolov and Miller, 2005). So in this section, FTIR-transmission analysis of the O-D stretching band was carried out to analyze the water structure of KCl, $\text{MgCl}_2 \cdot 6\text{H}_2\text{O}$ and $\text{KMgCl}_3 \cdot 6\text{H}_2\text{O}$ solutions prepared with the mixture of 4 wt. % D_2O in H_2O .

Since the O-D band peak position is highly sensitive to the water structure, small changes of water structure caused by the addition of a small amount of salt can be detected with an accuracy of 2 cm^{-1} . Then, comparing the results of the O-D band width, the changes in peak position provide an important metric about the effect of salts on water structure. So, in this paper, changes in the O-D band peak position were determined to analyze the interaction between salt ions and water molecules.

The peak position of the O-D band for KCl shifts to a higher wavenumber with an increase in KCl concentration when compared to the O-D band for the pure $\text{D}_2\text{O}/\text{H}_2\text{O}$ mixture, as shown in Fig. 3. The results obviously show that KCl is a structure breaker salt, which destroys the “ice-like” structure of water reflected in the region around 2380 cm^{-1} . The opposite tendencies are observed in solutions of bischofite and carnallite, in Fig. 4 and Fig. 5, respectively, which show that both bischofite and carnallite salts are structure maker salts which enhance the hydrogen bonded network between water molecules in the brine. Based on bubble attachment time measurements it seems that neither cationic nor anionic collectors are able to break the enhanced ice-like interfacial water structure and adsorb at the surfaces of bischofite and carnallite.

In the case of KCl and $\text{MgCl}_2 \cdot 6\text{H}_2\text{O}$, because of the common anion Cl^- it appears that a

structure breaking effect (Nickolov and Miller, 2005), is due to the different cations. Therefore, it is evident that K^+ has a structure breaking effect while Mg^{2+} definitely has a strong structure making effect. This conclusion is further confirmed by the results of the O-D stretching spectra of carnallite ($KMgCl_3 \cdot 6H_2O$) which is a double salt of KCl and $MgCl_2$. In the carnallite brine solution, K^+ and Mg^{2+} are in the solution at the same time. Though the effects of K^+ and Cl^- are water structure breaking, the structure making effect of Mg^{2+} is so strong that overcomes the structure breaking effects of K^+ and Cl^- , consequently carnallite still is classified as a water structure maker.

In order to better understand about the effects of these three salts on water structure, the wavenumber of O-D peak position for the solutions of sylvite, bischofite and carnallite are plotted in Fig. 6 versus the mole ratio of water to salt. In the case of the structure breaker, KCl, the peak wavenumbers for the O-D band increase, while the peak wavenumbers for the O-D band for the structure makers, bischofite and carnallite, decrease at higher salt concentrations, i.e. a lower mole ratio of water to salt. According to previous research (Nickolov and Miller, 2005), the solubility of the salts should be high enough so that the mole ratio of water to salt becomes less than ca. 20:1-10:1. In this case, the number of water molecules affected by the salt should be comparable with, or higher than, those of bulk-like water. Then the change in the shape of the O-D band in aqueous salt solutions affected by the structure making/breaking properties of the salt can be observed in detail. The shift of the O-D band peaknumber for KCl is greater than 14 cm^{-1} compared to 10 cm^{-1} and 5 cm^{-1} for $MgCl_2 \cdot 6H_2O$ and $KMgCl_3 \cdot 6H_2O$. Compared to the results of the bischofite solution, the shift of the O-D band for the carnallite brine is not very significant due to the presence of K^+ which has a structure breaking effect on the brine. Nevertheless the carnallite still exhibits a water structure making tendency. Again Mg^{2+} plays a dominant effect on water structure when compared to K^+ and Cl^- in carnallite brine.

3.3 Viscosity Measurements

Viscosity is a macroscopic parameter often used to classify soluble salts into structure makers and structure breakers. In general, salts with a structure making character increase the viscosity of solutions with an increase in salt concentration, while salts which decrease the viscosity of brine are considered to be structure breaker salts. Therefore measurements of the viscosity for KCl and $MgCl_2 \cdot 6H_2O$ brines at different concentrations were conducted to provide additional information about their water structure properties. Fig. 7 shows the relative viscosity values versus concentration for solutions of KCl and $MgCl_2 \cdot 6H_2O$. The viscosity of the KCl solutions shows a weak dependence on salt concentration, while the concentration of $MgCl_2 \cdot 6H_2O$ (from very dilute to 2.7 mol/L) has a significant influence on the relative viscosity of the brine, which changes from 1.0 to $\sim 2.7\text{ mPa}\cdot\text{S}$. It can be assumed that more and more free water

molecules were coordinated by Mg^{2+} with an increase in the Mg^{2+} concentration. The fraction of free water in the solution would decrease accordingly.

4. CONCLUSIONS

Bubble attachment time measurements suggest that both the cationic collector, ODA, and the anionic collector, SDS, adsorb at the KCl surface to create a hydrophobic state. Apparently neither collector adsorbs at the $MgCl_2 \cdot 6H_2O$ and $KMgCl_3 \cdot 6H_2O$ surfaces. Surface charge appears to have no effect on the flotation of these salts. Further, FTIR spectroscopy of aqueous solutions of these salts was used to reveal changes in the O-D stretching bands of water. The observed changes in the peak number of the O-D band reveal the fact that $MgCl_2 \cdot 6H_2O$ and $KMgCl_3 \cdot 6H_2O$ have a structure making effect on water leading to poor flotation with both cationic and anionic collectors. On the other hand, KCl has water structure breaking properties in aqueous solution and consequently it appears that collector adsorption is possible. The results from FTIR spectroscopy are further supported by viscosity measurements of salt brines which show that Mg^{2+} has a water structure making effect in contrast to K^+ which has a water structure breaking effect. Because the effect of Mg^{2+} on water structure is much stronger than K^+ , carnallite ($KMgCl_3 \cdot 6H_2O$) is still a structure maker salt in aqueous solutions. It is evident that Mg^{2+} plays an important role in defining the water structure in solutions of bischofite ($MgCl_2 \cdot 6H_2O$) and carnallite ($KMgCl_3 \cdot 6H_2O$). First of all, the hydration of Mg^{2+} is extremely strong and water molecules are extensively coordinated by the ion Mg^{2+} . The strength would not diminish through a single layer of water molecules and it may be extended to further distances. Further research with molecular dynamics simulations is in progress.

ACKNOWLEDGMENTS

The financial support provided by the Department of Energy, Basic Science Division Grant No. DE-FG-03-93ER14315, National Key Technology R&D Program China 2006BAB09B02 is gratefully acknowledged, the National Natural Science Foundation of Qinhai province (Grant No. 21010731) and the National Natural Science Foundation of China (Grant No. 20971081).

REFERENCES

- Burdukova, E., Laskowski, J.S., Effect of Insoluble Amine on Bubble Surfaces on Particle-Bubble Attachment in Potash Flotation. *The Canadian Journal of Chemical Engineering*, 2009, 87(3), 441-447.
- Burdukova, E., Laskowski, J.S., Forbes, G.R., Precipitation of dodecyl amine in KCl-NaCl saturated brine and attachment of amine particles to KCl and NaCl surfaces. *International Journal of Mineral Processing*, 2009, 93(1), 34-40.
- Cao, Q., Du, H., Miller, J.D., Wang, X., Cheng, F., Surface chemistry features in the flotation of KCl. *Minerals Engineering*, 2010, 23(5), 365-373.
- Cheng, F., Niu, Z., Li, C., Cheng, X., 2002. Phase diagrams of water-salt system and industry application. Tianjing University Publisher, pp. 61-63.
- Dillon, S., Dougherty, R., Raman studies of the solution structure of univalent electrolytes in water. *Journal of Physical Chemistry A*, 2002, 106(34), 7647-7650.
- Drelich, J., Miller, J.D., Good, R.J., The Effect of Drop (Bubble) Size on Advancing and Receding Contact Angles for Heterogeneous and Rough Solid Surfaces as Observed with Sessile-Drop and Captive-Bubble Techniques. *Journal of Colloid and Interface Science*, 1996, 179(1), 37-50.
- Du, H., Liu, J., Ozdemir, O., Nguyen, A.V., Miller, J.D., Molecular features of the air/carbonate solution interface. *Journal of Colloid and Interface Science*, 2008, 318(2), 271-277.
- Du, H., Miller, J.D., Interfacial Water Structure and Surface Charge of Selected Alkali Chloride Salt Crystals in Saturated Solutions: A Molecular Dynamics Modeling Study. *Journal of Physical Chemistry C*, 2007, 111(27), 10013-10022.
- Du, H., Rasaiah, J.C., Miller, J.D., Structural and Dynamic Properties of Concentrated Alkali Halide Solutions: A Molecular Dynamics Simulation Study. *Journal of Physical Chemistry B*, 2007, 111(1), 209-217.
- Finch, J.A., Smith, G.W., Dynamic surface tension of alkaline dodecylamine acetate solution in oxide flotation. *Trans. Institute of Mining and Metallurgy*, 1972, 81, C213-C218 (Sec. C)
- Foot, D.G., Huiatt, J.L., 1981. Direct flotation of potash from insoluble-slime-bearing sylvinitic and carnallite Ores, In *SME Annual Meeting*, Chicago, Illinois, pp. 22-26.
- Fuerstenau, D.W., Fuerstenau, M.C., Ionic size in flotation collection of alkali halides. *Transactions of the American Institute of Mining, Metallurgical and Petroleum Engineers*, 1956, 205(Tech. Publ. 4156-B), 302-306.
- García-Veigas, J., Rosell, L., Zak, I., Playà, E., Ayora, C., Starinsky, A., Evidence of potash salt formation in the Pliocene Sedom Lagoon (Dead Sea Rift, Israel). *Chemical Geology*, 2009, 265(3-4), 499-511.
- Hancer, M., Celik, M.S., Miller, J.D., The Significance of Interfacial Water Structure in Soluble Salt Flotation Systems. *Journal of Colloid and Interface Science*, 2001, 235(1), 150-161.
- Hancer, M., Miller, J.D., The flotation chemistry of potassium double salts: Schoenite,

- kainite, and carnallite. *Minerals Engineering*, 2000, 13(14-15), 1483-1493.
- Hancer, M., Sperline, R.P, Miller, J.D, Anomalous dispersion effects in the IR-ATR spectroscopy of water. *Applied Spectroscopy*, 2000, 54(1), 138-143.
- Huiatt, J.L., Tippin, R.B., Potter, G.M., 1975. Potassium salt flotation from great salt lake evaporites In *SME/AIME Transactions*, pp. 303-310.
- Jiang, J.W., Sandler, S.I., A new model for the viscosity of electrolyte solutions. *Industrial & Engineering Chemistry Research*, 2003, 42(25), 6267-6272.
- Kirby, J.E., 1936. Flotation process, USA. Patent No. 62377.
- Koneshan, S., Rasaiah, J.C., Lynden-Bell, R.M., Lee, S.H., Solvent Structure, Dynamic, and Ion Mobility in Aqueous Solutions at 25°C. *Journal of Physical Chemistry B*, 1998, 102(21), 4193-4204.
- Lai, R.W.M., Smith, R.W., On the relationship between contact angle and flotation behavior. *Trans. Am. Inst. Min. Eng*, 1966, 235, 413-418.
- Max, J.J., Chapados, C., Infrared spectroscopy of aqueous ionic salt mixtures at low concentrations: ion pairing in water. *The Journal of Chemical Physics*, 2007, 127(11), 114509-1-114509-10.
- Max, J.J., Chapados, C., Infrared spectroscopy of acetone-methanol liquid mixtures: Hydrogen bond network. *The Journal of Chemical Physics*, 2005, 122(1), 14504-1-14504-18.
- Miller, J.D., Yalamanchili, M.R., Kellar, J.J., Surface charge of alkali halide particles as determined by laser-Doppler electrophoresis. *Langmuir*, 1992, 8(5), 1464-1469.
- Nicholov, Z.S., Paruchuri, V., Shah, D.O., Miller, J.D., FTIR-ATR studies of water structure in reverse micelles during the synthesis of oxalate precursor nanoparticles. *Colloids and Surfaces A*, 2004, 232(1), 93-99.
- Nickolov, Z.S., Miller, J.D., Water structure in aqueous solutions of alkali halide salts: FTIR spectroscopy of the OD stretching band. *Journal of Colloid and Interface Science*, 2005, 287(2), 572-580.
- Nickolov, Z.S., Ozcan, O., Miller, J.D., FTIR analysis of water structure and its significance in the flotation of sodium carbonate and sodium bicarbonate salts. *Colloids and Surfaces A*, 2003, 224(1-3), 231-239.
- Ozdemir, O., Çelik, M.S., Nickolov, Z.S., Miller, J.D., Water structure and its influence on the flotation of carbonate and bicarbonate salts. *Journal of Colloid and Interface Science*, 2007, 314(2), 545-551.
- Robinson, G.W., Zhu, S.B., S.Singh, Evans, M.W., 1996. Water in Biology, Chemistry and Physics, In *World Scientific*, Singapore, pp. 113-114.
- Rogers, J., Flotation of soluble salts. *Bulletin - Institution of Mining and Metallurgy*, 1957, 607, 439-452.
- Roman, R.J., Fuerstenau, M.C., Seidel, D.C., Mechanisms of soluble salt flotation. I. *Transactions of the American Institute of Mining, Metallurgical and Petroleum Engineers*, 1968, 241(1), 56-64.
- Rosenbaum, J.M., Fuerstenau, D. W, Laskowsik, J.S., Effect of surface functional groups



- on the flotation of coal. *Colloids Surfaces*, 1983, 8(2), 153-173.
- Scherer, J., Go, M., Kint, S., Raman spectra and structure of water from -10 to 90. deg. *The Journal of Physical Chemistry*, 1974, 78(13), 1304-1313.
- Searls, J.P., 1990. *Minerals Year Book-1989*, p. 801.
- Titkov, S., Flotation of water-soluble mineral resources. *International Journal of Mineral Processing*, 2004, 74(1-4), 107-113.
- Ujike, T., Tominaga, Y., Mizoguchi, K., Dynamical structure of water in alkali halide aqueous solutions. *The Journal of Chemical Physics*, 1999, 110(3), 1558-1568.
- Veeramasuneni, S., Hu, Y., Miller, J.D., The surface charge of alkali halides: consideration of the partial hydration of surface lattice ions. *Surface Science*, 1997, 382(1-3), 127-136.
- Yalamanchili, M.R., Kellar, J.J., Miller, J.D., Adsorption of collector colloids in the flotation of alkali halide particles. *International Journal of Mineral Processing*, 1993, 39(1-2), 137-153.
- Ye, Y., Khandrika, S.M., Miller, J.D., Induction-time measurements at a particle bed. *International Journal of Mineral Processing*, 1989, 25(3-4), 221-240.
- Ye, Y., Miller, J.D., The significance of bubble/particle contact time during collision in the analysis of flotation phenomena. *International Journal of Mineral Processing* 1989, 25(3-4), 199-219.
- Zhelyaskov, V., Georgiev, G., Nickolov, Z.S., Miteva, M., Concentration Raman study of intramolecular, intermolecular and Fermi resonance interactions in the OH stretching spectra of dilute solutions of HDO in D₂O using Fourier deconvolution technique. *Molecular Physics*, 1988a, 64(6), 1133-1144,
- Zhelyaskov, V., Georgiev, G., Nickolov, Z.S., Miteva, M., Temperature study of intra-molecular coupling and Fermi resonance constants in the Raman spectra of liquid water using Fourier deconvolution. *Journal of Raman Spectroscopy*, 1988b, 19(6), 405-412.
- Zhu, X., Suhr, H., Shen, Y., Surface vibrational spectroscopy by infrared-visible sum frequency generation. *Physical Review B*, 1987, 35(6), 3047-3050.

CAPTIONS

Table captions

Table 1. The measured bubble attachment times for different concentrations of ODA/SDS at beds of sylvite (KCl) particles.

Figure captions

Figure. 1. The effect of contact time and ODA concentration on attachment between air bubble and Sylvite (KCl) particles (150-180 μ m) at room temperature and pH=6.

Figure. 2. The effect of contact time and SDS concentration on attachment between air bubble and sylvite (KCl) particles (150-180 μ m) t room temperature and pH=6.

Figure. 3. O-D stretching band spectra of solutions of sylvite (KCl) in 4 wt% D₂O in H₂O mixtures depending on concentration. The spectrum of the pure 4 wt% D₂O in H₂O mixtures is shown with a red line.

Figure. 4. O-D stretching band spectra of solutions of bischofite (MgCl₂•6H₂O) in 4 wt% D₂O in H₂O mixtures depending on concentration. The spectrum of the pure 4 wt% D₂O in H₂O mixtures is shown with a red line.

Figure. 5. O-D stretching band spectra of solutions of carnallite (KMgCl₃•6H₂O) in 4 wt% D₂O in H₂O mixtures depending on concentration. The spectrum of the pure 4 wt% D₂O in H₂O mixtures is shown with a red line.

Figure. 6. Dependencies of the OD band peak wavenumbers in solutions of sylvite (KCl), carnallite (KMgCl₃•6H₂O) and bischofite (MgCl₂•6H₂O) in 4 wt.% D₂O in H₂O mixtures depending on mole ratio water: salt.

Figure. 7. Viscosity of sylvite (KCl) and bischofite (MgCl₂•6H₂O) solutions as a function of concentration at 23°C.

Table 1. The measured bubble attachment times for different concentrations of ODA/SDS at beds of sylvite (KCl) particles.

ODA concentration (M)	Attachment time (ms)	
	ODA	SDS
No collector	2000	2000
1×10^{-6}	1700	1800
5×10^{-6}	600	-
8×10^{-6}	60	190
1×10^{-5}	50	100
5×10^{-5}	-	37

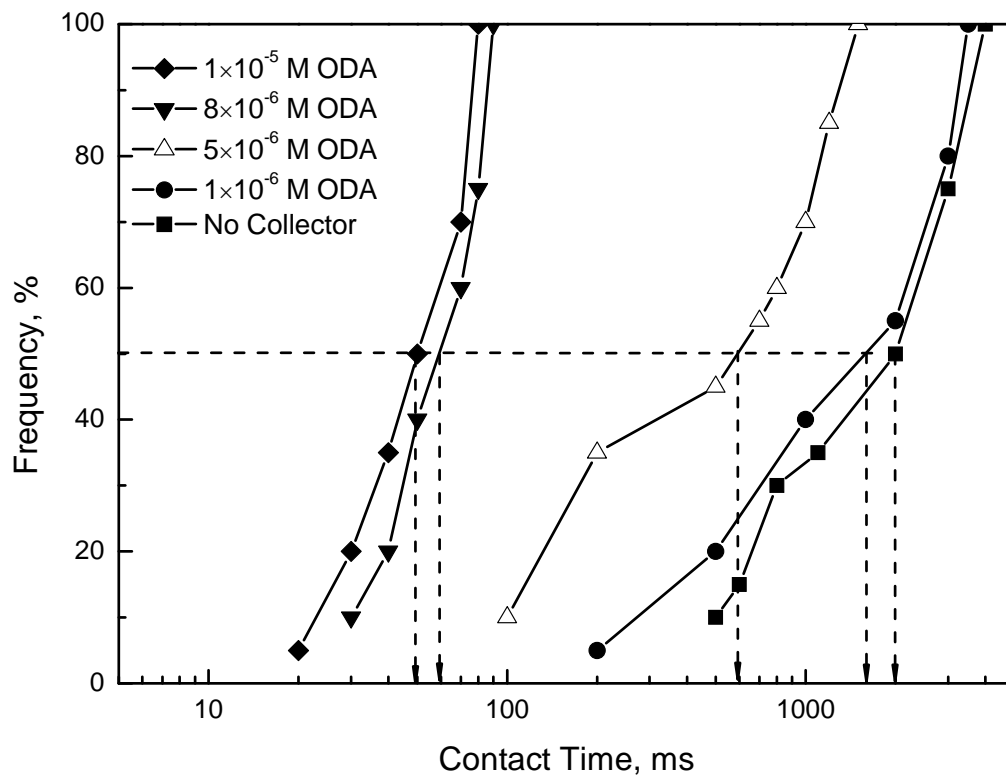


Figure 1. The effect of contact time and ODA concentration on attachment between air bubble and Sylvite (KCl) particles (150-180 μ m) at room temperature and pH=6.

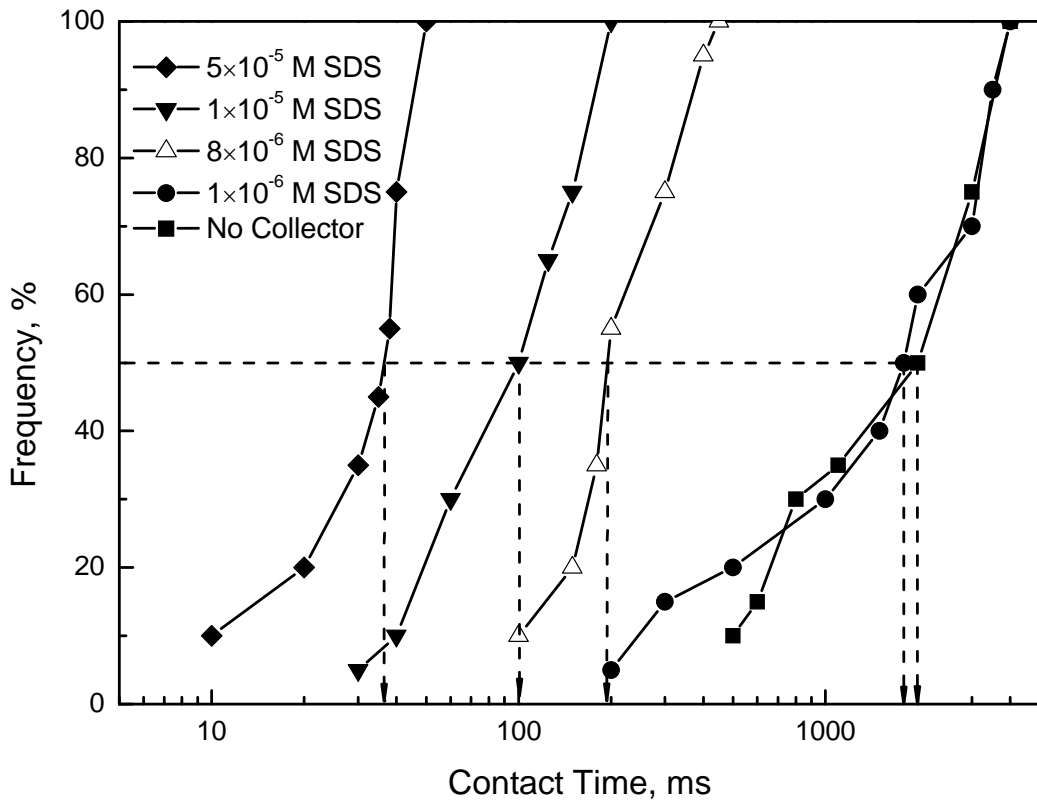


Figure 2. The effect of contact time and SDS concentration on attachment between air bubble and sylvite (KCl) particles (150-180 μ m) at room temperature and pH=6.

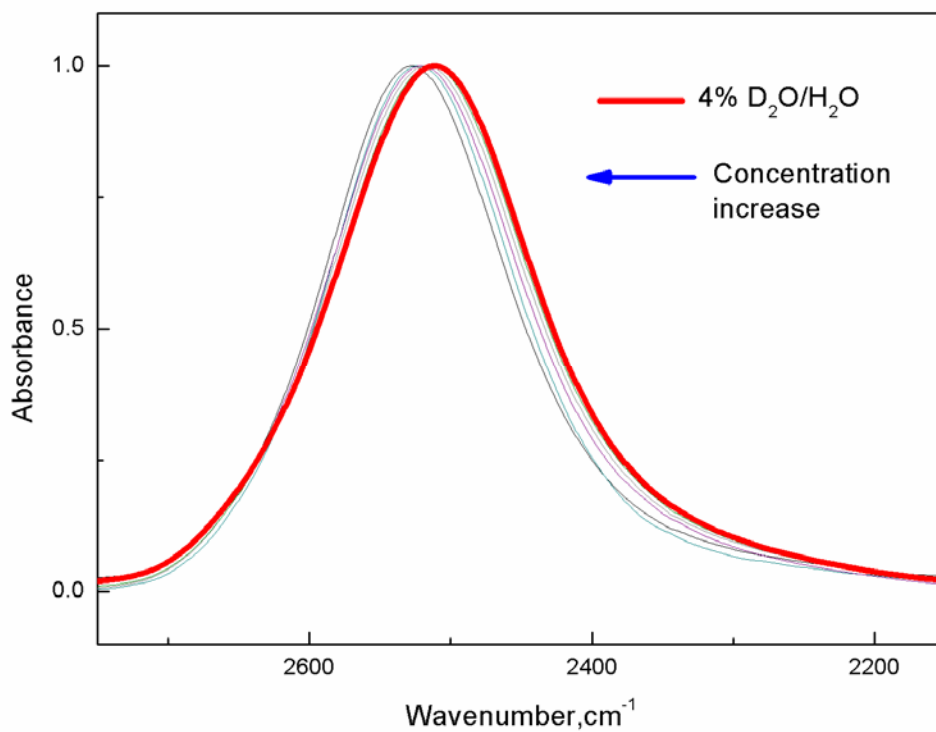


Figure 3. O-D stretching band spectra of solutions of sylvite (KCl) in 4 wt% D₂O in H₂O mixtures depending on concentration. The spectrum of the pure 4 wt% D₂O in H₂O mixtures is shown with a red line.

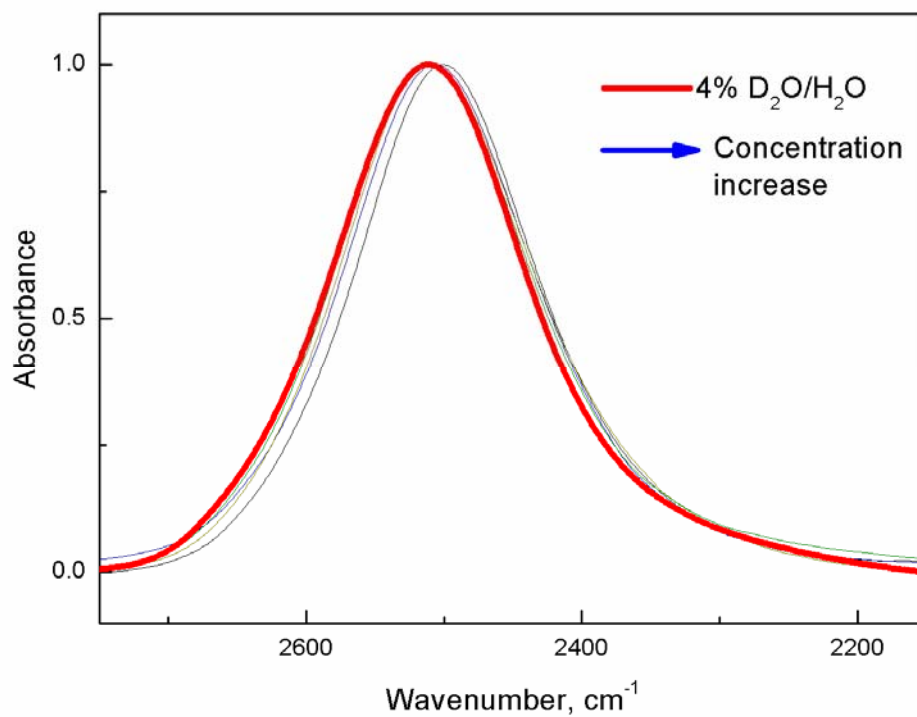


Figure 4. O-D stretching band spectra of solutions of bischofite ($\text{MgCl}_2 \cdot 6\text{H}_2\text{O}$) in 4 wt% D_2O in H_2O mixtures depending on concentration. The spectrum of the pure 4 wt% D_2O in H_2O mixtures is shown with a red line.

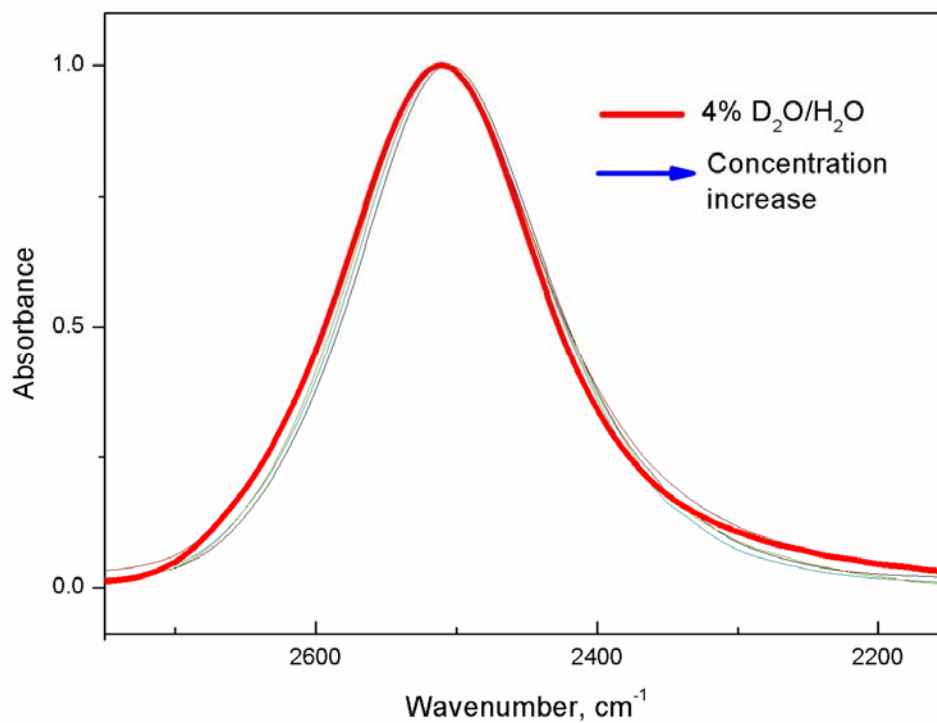


Figure 5. O-D stretching band spectra of solutions of carnallite ($\text{KMgCl}_3 \cdot 6\text{H}_2\text{O}$) in 4 wt% D_2O in H_2O mixtures depending on concentration. The spectrum of the pure 4 wt% D_2O in H_2O mixtures is shown with a red line.

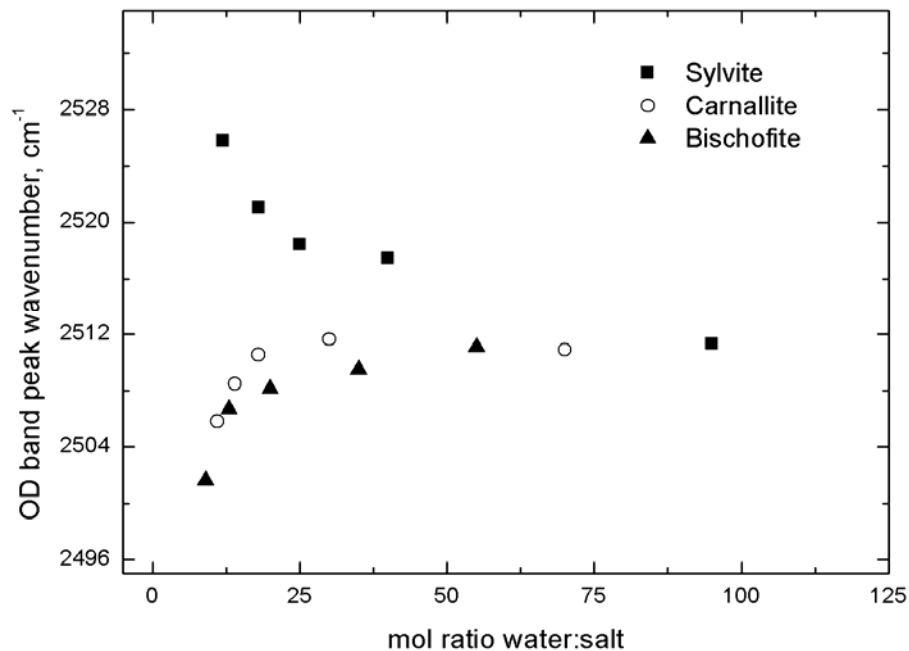


Figure 6. Dependencies of the OD band peak wavenumbers in solutions of sylvite (KCl), carnallite ($\text{KMgCl}_3 \cdot 6\text{H}_2\text{O}$) and bischofite ($\text{MgCl}_2 \cdot 6\text{H}_2\text{O}$) in 4 wt.% D_2O in H_2O mixtures depending on mole ratio water: salt.

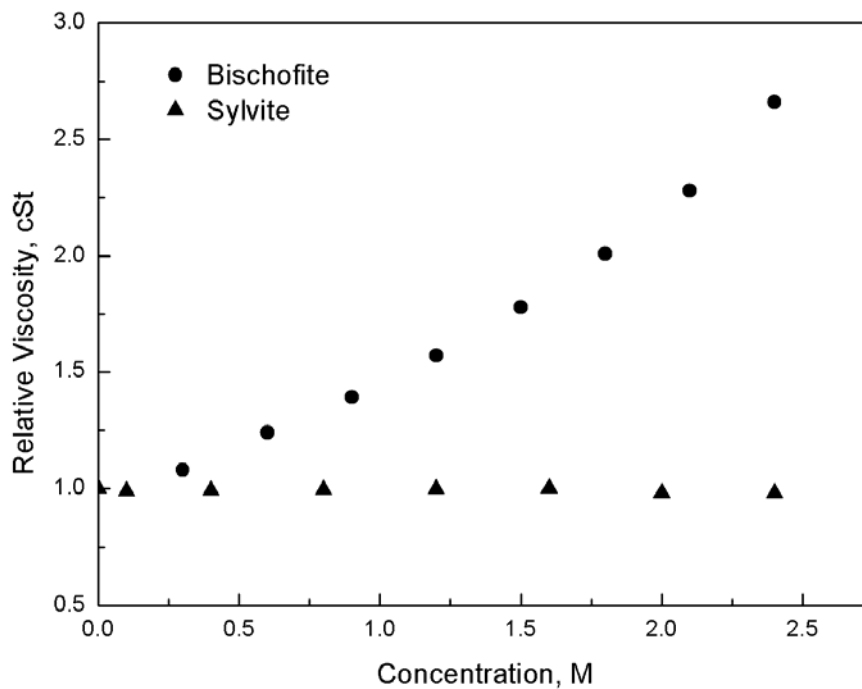


Figure 7. Viscosity of sylvite (KCl) and bischofite ($\text{MgCl}_2 \cdot 6\text{H}_2\text{O}$) solutions as a function of concentration at 23°C.